Physics – Uspekhi **64** (10) 1038 – 1048 (2021)

PHYSICS OF OUR DAYS

PACS numbers: 06.20.Jr, 06.30.Ft, 12.20.Fv, 32.10.Fn, 32.30.Jc, 42.62.Fi

Proton charge radius

K Yu Khabarova, N N Kolachevsky

DOI: https://doi.org/10.3367/UFNe.2021.06.038986

Contents

Abstract. The so-called proton charge radius puzzle was one of the challenging problems in physics in the last decade. A significant (at the level of four standard deviations (4σ)) difference between the values of the root-mean-square proton charge radius measured in normal and muonic hydrogen has kindled lively discussions among both experimentalists and theoreticians specializing in quantum electrodynamics. The problem becomes even more glaring (up to 7σ) if data on the scattering of electrons on protons are taken into account. We review various methods that enable measurement of the proton charge radius, analyze the origin of the disagreement, and present results of recent experiments that aim at resolving this puzzle.

Keywords: proton radius, hydrogen atom, muonic hydrogen, proton radius puzzle, Rydberg constant, single-photon spectroscopy, e–p scattering

1. Introduction

The history of the proton charge radius (r_p) begins with experiments on the scattering of high-energy electrons on protons that aimed at studying the electromagnetic structure of the proton and neutron. The experimental landscape was later complemented by experiments on the high-precision radio frequency and laser spectroscopy of the hydrogen atom, which independently yielded the value of r_p. The importance of this constant for fundamental physics is explained, in particular, by the fact that it is the source of the most significant error in the Rydberg constant (the coefficient of correlation between these two constants is 98.9%). The Rydberg constant $R_\infty = m_e c\alpha^2/(2h)$, where h is the Planck constant, m_e is the electron mass, c is the speed of light in a vacuum, and α is the fine-structure constant, is, in turn, the coefficient of conversion between the atomic system of units and the SI system and is a basic component in determining many other fundamental constants.

Another independent method to determine the proton charge radius was designed and implemented at the Paul Scherrer Institute (PSI, Switzerland). This method involved a highly-sensitive experiment on the spectroscopy of exotic muonic hydrogen, μp, which is a bound system that consists of a proton and negatively charged muon. A muon is a lepton similar to the electron, owing to which standard methods of quantum electrodynamics (QED) for bound systems can be applied. However, the muon is 207 times heavier than the electron, and, consequently, the Bohr radius of the muon is $a_0/207$, where $a_0 = \hbar/(m_e c\alpha)$ is the Bohr radius of the electron. Consequently, the corrections due to overlapping of the $|\psi(0)|^2$ wave function with the nucleus, which are proportional to $\psi(\mathbf{r})$, are enhanced by many orders of magnitude. Although the muon lifetime is only 2 μs, it is possible to measure the Lamb shift using the laser spectroscopy technique at a wavelength of 6 μm and improve the accuracy of the r_p value by an order of magnitude.

Similar to other fundamental constants, the 'tabular' value of the proton radius is set by the Committee on Data for Science and Technology (CODATA), whose mission is to reconcile the values of constants taking into consideration errors in various experiments and correlations among them [1]. However, experiments with muonic hydrogen carried out in 2010 yielded a surprising result that disagreed with both the

K Yu Khabarova [(1,a)], **N N Kolachevsky** [(1,2)]
[(1)] Lebedev Physical Institute, Russian Academy of Sciences, Leninskii prosp. 53, 119991 Moscow, Russian Federation
[(2)] International Center for Quantum Optics and Quantum Technologies (Russian Quantum Center), ul. Novaya 100, 143025 Skolkovo, Moscow region, Russian Federation
E-mail: [(a)] kseniakhabarova@gmail.com

Received 11 February 2021, revised 4 June 2021
Uspekhi Fizicheskikh Nauk **191** (10) 1095 – 1106 (2021)
Translated by M Zh Shmatikov

data obtained in experiments with normal hydrogen and electron scattering. The disagreement, which was significant (about 7σ), indicated the existence of a profound problem and did not allow the results of experiments of the three types to be correctly averaged. The so-called proton radius puzzle emerged. A number of hypotheses that could explain the nature of the observed disagreement were suggested, beginning with errors in the experiments and ending with the incompleteness of the Standard Model. To find a solution to the puzzle, theoretical studies were carried out in which a 'new physics' was searched for and experiments were conducted which were supposed to shed light on the problem.

However, experiments with muonic deuterium carried out in 2016 at PSI yielded again a significant (7.5σ) disagreement between the charge radius of the deuteron r_d and the radius of a normal deuteron. As a result, the charge radius puzzle became even more perplexing. Two sets of internally consistent results were available, which pertained to electronic systems (normal hydrogen and electron scattering) and muonic systems. The suspicion arose that the behavior of the muon and its interaction with a charged center are not fully described by QED methods, and there are some additional corrections which are only characteristic of muonic systems. Attention is attracted by the correction needed in theoretical calculations in muonic systems, which is 140σ for μp and 22σ for μd.

However, the disagreements observed might be well explained by simpler reasons within the modern physical paradigm and originate in the employed experimental techniques and data processing methods. In the case of electron scattering on protons, model errors in the extrapolation of the momentum transferred to the nucleus may fairly easily explain the observed disagreement. No less probable are problems unaccounted for in spectroscopic experiments with normal hydrogen: the required adjustment equal to 4σ may occur as a result of incorrect determination of the centers of corresponding spectral lines. It should be noted that, for spectrally broad lines of transitions to the excited states of normal hydrogen (3S, 4P, 8D, etc. with a characteristic linewidth of $\sim$ 10 MHz), the required correction only corresponds to the error equal to 1/1000 of the linewidth. This option also exists in muonic experiments, but then one must 'miscalculate' by 1/4 of the spectral width of the line.

This simple analysis clearly shows that a solution to the proton radius puzzle without new experiments based on advanced techniques is an extremely challenging if not impossible task. Special attention should be paid to experiments with normal hydrogen and, possibly, scattering experiments. The scientific community has been intrigued for almost a decade by the mysterious proton. However, what is the root of the puzzle? Is it due to experimental errors or a new, yet unexplored area of physics?

2. What is the proton charge radius?

It has been known for a long time that the proton is not a pointlike particle, but its diameter is of the order of 10^{-15} m. It was found in the 1950s that the proton has an internal structure. Experiments on the scattering of high-energy electrons on proton-containing targets, which were carried out by Robert Hofstadter, showed that the results observed differ from the scattering laws inherent to pointlike nuclei [4]. Hofstadter was awarded with the Nobel Prize in physics in 1961 for his discoveries in the area of nucleon structure.

Prior to this discovery, the proton was considered to be a particle that has a pointlike charge and a pointlike magnetic moment. Should this description be correct, scattering of an electron on a proton would have been described by the formula derived by Rosenbluth, which we quote in its original form [3]:

$$\left(\frac{\mathrm{d}\sigma}{\mathrm{d}\Omega}\right)_{\text{Rosenbluth}} = \sigma_{\text{NS}}\left\{1 + \frac{\hbar^2 q^2}{4M^2c^2}\left[2\left(1+k\right)^2 \tan^2\frac{\theta}{2} + k^2\right]\right\}, \tag{1}$$

where

$$\sigma_{\text{NS}} = \left(\frac{\mathrm{d}\sigma}{\mathrm{d}\Omega}\right)_{\text{Mott}} = \left(\frac{e^2}{2E_0}\right)^2 \frac{\cos^2(\theta/2)}{\sin^4(\theta/2)} \times \frac{1}{1 + \left[2E_0/(Mc^2)\right]\sin^2(\theta/2)}, \tag{2}$$

$$q = \frac{2E_0}{\hbar c}\,\frac{\sin(\theta/2)}{\sqrt{1 + \left[2E_0/(Mc^2)\right]\sin^2(\theta/2)}}. \tag{3}$$

Here, σ_{NS} is the differential cross section of Mott scattering, $\theta \in \{0, \pi\}$ is the scattering angle in the laboratory system, E_0 is the energy of the impinging electron in the laboratory system, M is the proton mass, $k = 1.79$ corresponds to the anomalous part of the magnetic moment of the proton, and q^2 is the four-momentum vector squared, which corresponds to the virtual photon of electromagnetic interaction between the electron and the proton [5]. It may be noted that the very existence of the anomalous (non-Dirac) part of the magnetic moment of the proton is an indication of its structure, i.e., finite dimensions.

Experiments on the scattering of 188-MeV electrons on hydrogen atoms [6, 7] were the first to show that the proton's dimensions should be nonzero. Experimental points in the case of large scattering angles proved to be located lower than the theoretical curve that follows from the Rosenbluth formula (Fig. 1). Figure 1 also displays for comparison the curve of the Mott scattering σ_{NS}. It is of importance that, for a smaller electron energy (100 MeV), when the effects related to proton size are expected to be small, the angular scattering distribution fairly satisfactorily follows the Rosenbluth scattering law, thus precluding possible experimental errors [7]. It was found in this way that the proton has a distributed charge.

It also became clear that the distributed nature of proton charge should also distort the Coulomb potential that determines energy levels in atoms. S-states, whose wave function does not vanish at the origin of coordinates, are the most sensitive to this distortion of the potential.

Concurrently with Hofstadter's pioneering experiments, elastic scattering of electrons from the nucleon was theoretically analyzed using the Feynman diagram technique. It was assumed that the contribution from the Born term dominates due to the smallness of electromagnetic interaction constant α. Basic expressions have been derived for hadronic currents, and two invariant form factors, F_1 and F_2, have been introduced, which were named later the Dirac and Pauli form factors. Following Rosenbluth's approach [9], Yennie, Levy, and Ravenhall [8] derived in 1957 a formula for e–p-scattering that contains these two form factors. Experimental data can be analyzed in a more convenient way using another set of form

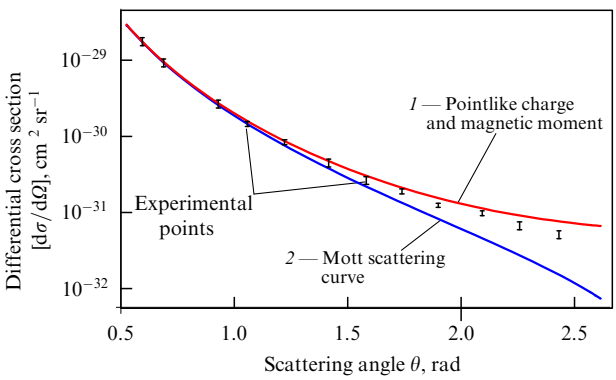

Figure 1. Angular distribution in the scattering of electrons on protons. If proton charge and magnetic moment were pointlike, the scattering diagram corresponding to the Rosenbluth model (curve *1*) would be expected (see formula (3)). Experimental points (experiment on scattering of electrons on a gaseous hydrogen target [7]) are located below curve *1*, thus confirming that charge in the proton is not pointlike. Displayed for comparison is curve *2* that corresponds to the Mott scattering in the model of a pointlike proton with charge $+e$ and without a magnetic moment.

factors, G_E and G_M [10, 11], which are related to F_1 and F_2 by the following formulas:

$$G_E = F_1 - \tau F_2 \,, \tag{4}$$

$$G_M = F_1 + F_2 \,. \tag{5}$$

Here, $\tau = Q^2/(4M^2) > 0$ is a quantity that depends on the transferred momentum, which in turn is defined as $Q^2/(2M) = -q^2/(2M) = E_0 - E_1$, where E_1 is the energy of the scattered electron. The differential cross section can be represented in this case as follows:

$$\frac{d\sigma}{d\Omega} = \left[\frac{e^2}{2E_0 \sin^2(\theta/2)}\right]^2 \frac{E_1}{E_0} \times \left(\frac{G_E^2 + \tau G_M^2}{1+\tau}\cos^2\frac{\theta}{2} + 2\tau G_M^2 \sin^2\frac{\theta}{2}\right). \tag{6}$$

The first part of the formula is the Rutherford cross section, the second ratio is related to the recoil effect, and the third term consists of two terms: (1) electric/magnetic scattering with consideration for the proton structure and (2) the magnetic part related to spin. The form factors in the $Q^2 \ll 1$ approximation can be represented as Fourier images of charge distribution $\rho(\mathbf{r})$ and magnetic moment $\mu(\mathbf{r})$, respectively:

$$G_E(Q^2) \approx G_E(\mathbf{Q}^2) = \int_{\text{vol}} \rho(\mathbf{r}) \exp(\mathrm{i}\mathbf{Q}\mathbf{r})\, d^3\mathbf{r} \,, \tag{7}$$

$$G_M(Q^2) \approx G_M(\mathbf{Q}^2) = \int_{\text{vol}} \mu(\mathbf{r}) \exp(\mathrm{i}\mathbf{Q}\mathbf{r})\, d^3\mathbf{r} \,. \tag{8}$$

If $Q \to 0$, the form factors should take the values $G_E(0) = 1$ and $G_M(0) = 2.79$. The latter quantity is equal to the magnetic moment of the proton measured in nuclear magneton units. Experiments at higher energies (5–20 GeV) showed, in turn, that the charge distribution $\rho(r)$ is best described by an exponential formula,

$$\rho(r) = \rho_0 \exp\left(-\frac{r}{a}\right), \tag{9}$$

where $a \approx 0.24$ fm. This model is currently generally adopted. The distribution of the magnetic moment is the same as the charge distribution, so $G_M(Q^2) = 2.79\, G_E(Q^2)$.

The proton charge radius is extracted in experiments on elastic e–p-scattering from the electric form factor $G_E(Q^2)$ as a function of the momentum transferred Q^2. Equation (6) shows that, if $Q^2 \ll 1$, the cross section of the elastic scattering can be represented as the product of the Mott cross section for a pointlike electron with spin 1/2 and the Fourier transform of the proton charge density:

$$\frac{d\sigma}{d\Omega} \approx \sigma_{\text{Mott}}\, G_E^2(Q^2) \,. \tag{10}$$

The following formula [15] holds in the Born approximation for a centrally symmetrical distribution integrated over angles

$$G_E(Q^2) = 1 + \sum_{n \geqslant 1} \frac{(-1)^n}{(2n+1)!} \langle r^{2n} \rangle Q^{2n} = 1 - \frac{1}{6} Q^2 \langle r^2 \rangle + \frac{1}{120} Q^4 \langle r^4 \rangle + \ldots \,, \tag{11}$$

which follows from the expansion in Fourier integral (7) by the rQ parameter. It can be seen that the expansion only contains average values of an even power of r:

$$\langle r^{2n} \rangle = \int r^{2n} 4\pi r^2 \rho(r)\, dr \,. \tag{12}$$

Equation (11) shows that, having measured the electric form factor, the value of $\langle r^2 \rangle$ can be extracted in a model independent way (i.e., without using any model of charge distribution).

The root-mean-square proton radius defined as $r_E = \sqrt{\langle r^2 \rangle}$ can be found from Eqn (11) when the transferred momentum tends to zero:

$$r_E = \sqrt{-\frac{6\hbar^2}{G_E(0)} \left.\frac{dG_E(Q^2)}{dQ^2}\right|_{Q^2=0}} \,. \tag{13}$$

The term 'proton radius' r_p is used in the literature; it is set equal to the root-mean-square charge radius $r_p = r_E$ and is approximately 0.8 fm.

This implies that experimental data for $G_E(Q^2)$ should be extrapolated to the zero value of the transferred momentum Q^2 and the slope of the tangent at $Q^2 = 0$ should be determined as shown in Fig. 2. The following problem, which emerges in processing experimental data, should be noted. Although theoretically $G_E(0) = 1$, the form factor cannot be directly measured in experiment. It is calculated by means of the Rosenbluth formula using differential cross sections and, consequently, it is determined with an error: $G_E^{\text{exp}}(0) = 1 \pm \delta$. In processing the data, an additional normalization parameter a_G is introduced, which turns out to be close to one. Thus,

$$\left.\frac{dG_E(Q^2)}{dQ^2}\right|_{Q^2=0} = -\frac{\langle r_E^2 \rangle}{6\hbar^2 a_G} \,. \tag{14}$$

For r_p to be determined with an accuracy of 1%, the cross section should be measured with the maximum accuracy possible with the correct normalization of experimental points. The accuracy with which cross sections are determined is limited by the accuracy in determining the absolute luminosity, which, is turn, is limited by the error in

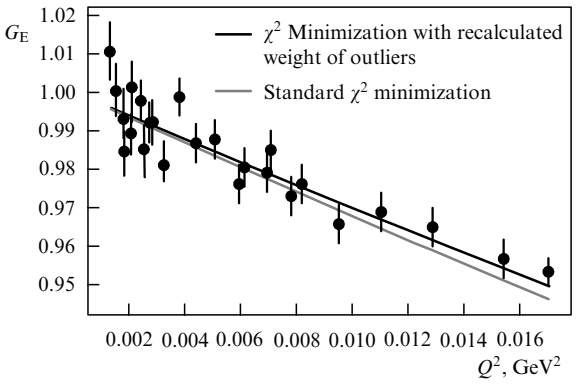

Figure 2. Approximation of data on e–p-scattering by various methods using a model with one fitting parameter. Approximation yields for the standard χ^2 minimization proton charge radius $r_p = 0.874$ fm. Fitting function with a reduced weight of outliers yields a value of 0.844 fm. (Plot is taken from Ref. [13].)

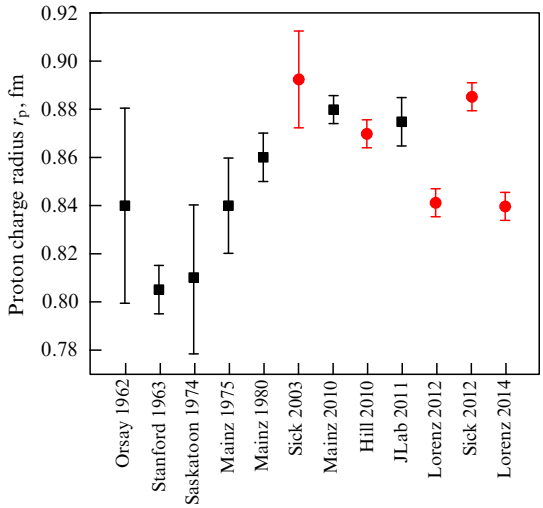

Figure 3. Proton charge radius obtained from experiments on electron-proton scattering. Squares show results of experiments carried out at the Linear Accelerator Laboratory (Orsay, France) [16] (1962), Cyclotron Laboratory of Harvard University (USA) [17] (1963), Accelerator Laboratory (Saskatoon, Canada) [18] (1974), Institute for Nuclear Physics of Mainz University (Germany) [19–21] (1975, 1980, 2010), and Jefferson Laboratory (JLab) (USA) [22]. Dots represent results of the re-analysis of experimental data using alternative approximating functions (displayed in the figure is the name of the first author or laboratory and the year of publication) [23–27].

determining the target density and electron beam intensity [12].

The main sources of systematic errors in scattering experiments are related to the normalization of experimental data that takes into account detection efficiency, purity of target, luminosity, and radiation effects. Most experiments used magnetic spectrometers which registered either the scattered electron and/or recoiled proton in a solid CH_n target or in a liquid or gaseous hydrogen target. The correlation method and back tracing of detected particles were used to separate the useful signal in elastic scattering from background processes. The luminosity determined by the beam intensity and density of the target was monitored using an additional detector. It is this detector that ensured relative normalization of data obtained at different values of the angle or energy but the same value of momentum transferred Q^2.

Significant attention has been paid in recent experiments on e–p-scattering to normalization issues, and the corresponding systematic errors are controlled at a level of several tenths of a percent [12]. However, earlier experiments lacked such stringent normalization criteria, and unification of different data sets proved to be problematic.

One of the methods to analyze data is to approximate experimental values with a function which includes the normalization factor a_G as a fitting parameter. In this approach, the normalization systematics prove to be included in the approximation error. However, study [13] showed that such processing can under certain circumstances significantly affect the final result. Moreover, even if a model with a single fitting parameter is chosen, the result obtained can depend on taking into account in the approximation individual data errors (see Fig. 2).

Given the strong dependence of the Mott cross section on the scattering angle and taking into account that the relative contribution of the form factors varies with changes in Q^2, the e–p-scattering method is arguably the most complicated method for analyzing the proton structure [14]. The accuracy in determining the proton charge radius in such experiments is no better than 1%. Figure 3 shows results for the proton charge radius obtained in experiments on e–p-scattering carried out over the last several decades. The earliest data were obtained in the experiments at Orsay [16], Stanford [17], Saskatoon [18], and Mainz [19, 20].

3. Determination of the proton charge radius in hydrogen atom spectroscopy

Spectral studies of the hydrogen atom, which played a decisive role in the birth of quantum mechanics and QED in the early 20th century, remain today of importance with regard to problems related to determining fundamental constants and testing basic theories. The energy levels of hydrogen are described in terms of the QED for bound states as a product of the Rydberg constant $\mathrm{Ry} = hcR_\infty$ and a complex dimensionless function. The Rydberg constant $\mathrm{Ry} = mc^2\alpha^2/2$ is, essentially, a coefficient for conversion of atomic units of measurement into the SI system, which relates the energy levels of model Bohr hydrogen to the hyperfine splitting of the ground state of cesium-133 atoms.

The dimensionless function, in turn, primarily depends on the fine structure constant α, the ratio of masses of the electron and the proton m_e/M, and the proton charge radius r_p:

$$E_{nlj} = hcR_\infty\left(-\frac{1}{n^2} + f_{nlj}\left(\alpha, \frac{m_e}{M}, \ldots\right) + \frac{C_{NS}}{n^3}\delta_{l0}\langle r_p^2\rangle\right), \quad (15)$$

where n, l, and j are the quantum number of the level (principal quantum number, orbital quantum number, and total momentum of the electron). The second term is a correction to the Bohr energy, $f_{nlj}(\alpha, m_e/M, \ldots) = X_{20}\alpha^2 + X_{30}\alpha^3 ln(\alpha) + X_{40}\alpha^4 + \ldots$, which includes relativistic corrections, recoil-related corrections, and corrections calculated in QED (eigenenergy, vacuum polarization, etc.) [28]. The last term in Eqn (15), which contains the C_{NS} factor, is the main correction related to the finite value of the proton charge radius r_p. Corrections of higher orders, which are due to the charge distribution in the nucleus, etc., are contained in $f_{nlj}(\alpha, m_e/M, \ldots)$.

It should be noted that Eqn (15) contains, in addition to the Rydberg constant and the proton charge radius, the fine structure constant α (the leading term $\sim \alpha^2$) and the mass ratio m_e/M (the leading term m_e/M). The α constant is known with a relative accuracy of 1.5×10^{-10} [29] and the mass ratio, 6×10^{-11} [30]. It is of importance that both values are determined in independent experiments. Consequently, the error introduced by these constants in Eqn (15) is at the level of the 14th decimal point and actually does not contribute in comparison with the accuracy of QED calculations, to say nothing about the accuracy of r_p.

Thus, spectroscopic experiments with the hydrogen atom enable determining R_∞ and r_p, which prove to be strongly correlated. To determine them jointly, the energy difference should be measured with the highest accuracy possible between (no fewer than) two pairs of levels with different principal quantum number n. It is natural and reasonable to choose as such an experiment the high-precision measurement of the frequency of the 1S–2S transition (two-photon transition, $\lambda = 243$ nm, intrinsic line width 1.3 Hz), which is known with a relative error of 4×10^{-15}. Hydrogen has no other metastable levels apart from the 2S state; all other transitions are much broader (~ 10 MHz) and measured with a significantly inferior accuracy.

The correction to energy levels due to the finite radius of the proton in Eqn (15) is described using the same logic as in the expansion of a form factor taking into consideration the finite charge distribution. The correction δV to the Coulomb potential V can be represented as [31]

$$\delta V = \frac{1}{6}\langle r_p^2\rangle \Delta V = \frac{2\pi}{3}\alpha\langle r_p^2\rangle \delta(\mathbf{r})\,. \tag{16}$$

Consequently, the correction to the atomic-level energy is

$$\Delta E_{n,l} = \mathrm{Ry}\,\frac{4m_r^3\alpha^2}{3m_e^3\lambda\!\!\!^{-2}_C n^3}\langle r_p^2\rangle \delta_{l0}\,, \tag{17}$$

where m_r is the reduced electron mass and $\lambda\!\!\!^{-}_C$ is the Compton wavelength. The correction related to the proton radius, which is approximately 1.25 MHz for the 1S hydrogen level, makes up a small fraction of the Lamb shift L_{1S} of the ground state. This correction is conventionally included in the expression for the Lamb shift. The following formulas [34],

$$L_{1S} = 8171.696(4)\ \mathrm{MHz} + 1.5639\langle r_p^2\rangle\ \mathrm{MHz}\,, \tag{18}$$

$$L_{2S} = 1057.694(2)\ \mathrm{MHz} + 0.1955\langle r_p^2\rangle\ \mathrm{MHz}\,, \tag{19}$$

hold where all QED contributions are taken into account and r_p^2 is measured in [fm^2] units. These formulas clearly show that, to determine r_p with an accuracy of 1%, the level energy should be measured with an accuracy of no less than 5 kHz. In contrast to L_{1S}, which is actually a 'virtual' quantity, the Lamb shift for the 2S state $L_{2S} \approx L_{1S}/8$ can be measured using radio-frequency spectroscopy techniques. Measurements of the Lamb shift do not provide an accurate value of the Rydberg constant but enable the extraction of r_p, which is one of the methods by which the proton charge radius can be determined.

Beginning in the late 1970s and until 2010, both the Lamb shift and the energies of optical transitions in the hydrogen atom (Fig. 4) were measured in numerous experiments. A list of the most accurate experiments of that period includes direct measurements of L_{2S} performed by Pipkin and Lundeen [35], determination of the Lamb shift based on the measured frequency of the $2S_{1/2} \to 2P_{3/2}$ transition using a theoretically calculated fine splitting of the 2P level [36], and an experiment in which the anisotropy of the emitted light in an external electric field was measured [37]. Distinguished in the spectroscopy of optical transitions is Biraben's Paris-based team, which has carried out since 1983 experiments on the spectroscopy of two-photon $2S-nS$ and $2S-nD$ transitions and the 1S–3S transition [38].

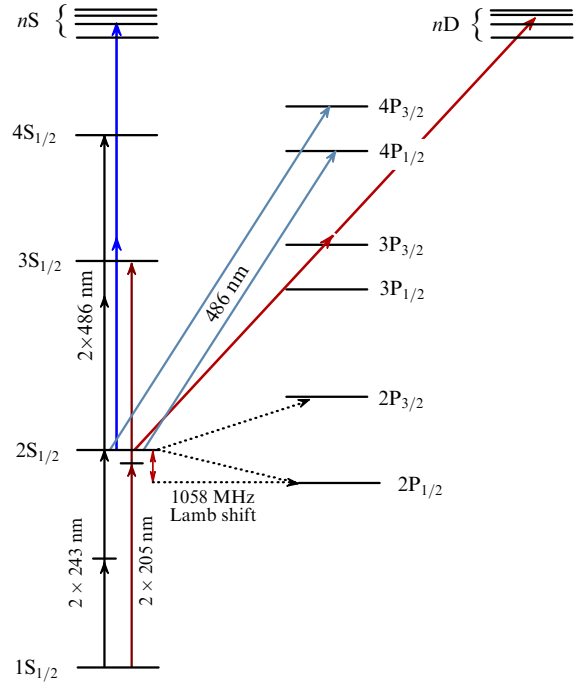

Figure 4. Transitions between energy levels of the hydrogen atom (not to scale) that were used to determine the proton charge radius and Rydberg constant. Dotted arrows show RF transitions. Corresponding results in determining r_p are displayed in Fig. 8.

By the beginning of the 21st century, global data obtained from hydrogen atom spectroscopy (both optical and radio frequency) provided an accuracy in the determination of r_p at a level of 0.5% and were in good agreement with data on e–p-scattering. This area of studies stagnated from 2000 through 2010: no new methods that could ensure a higher accuracy of measurements were suggested, while further refinement of QED calculations was senseless due to the error introduced by r_p. New experimental techniques substantially different from those described above were urgently needed.

4. Lamb shift in muonic hydrogen

The idea to measure the Lamb shift in muonic hydrogen is about 40 years old, but it was only in the early 2000s that a team of Germany- and Switzerland-based researchers commenced its practical implementation to obtain a more accurate value of the proton charge radius [32]. The μp atom is unstable; however, the muon lifetime (2 μs) is long enough to enable fairly accurate spectroscopic experiments. For example, the spectroscopy of muonium μe was realized in 1999 [33].

Due to the small Bohr radius of the muon ($a_0/207$), nucleus-related effects in muonic hydrogen prove to be enhanced by many orders of magnitude, a factor which significantly affects the Lamb shift structure. The table

Table. Contributions to Lamb shift L_{2S} in normal (ep) and muonic (μp) hydrogen.

L_{2S}	Radiative correction	Vacuum polarization	Contribution of r_p	Total shift
ep	1085 MHz	−27 MHz	0.14 MHz	1057 MHz
μp	0.1 THz	−45 THz	0.93 THz	−49 THz

displays a comparison of some contributions to the Lamb shift in normal and muonic hydrogen. Due to the change in the energy scale in μp, the Lamb shift in muonic hydrogen falls in the infrared range (6 μm), which opens prospects for laser spectroscopy. The shift structure substantially differs from that in normal hydrogen with regard to both radiative corrections (eigenenergy) of the lepton and effects related to the nucleus. The contribution of radiative corrections in the case of muons is small (virtual photons insignificantly 'spread' heavy muons), but the vacuum polarization effect proves to be dominant, since the Bohr orbit of the muon proves to be smaller than the Compton wavelength of the electron $\lambda_C \approx a_0/20$ which determines the thickness of the virtual polarized electron-positron cloud surrounding the proton. The contribution related to r_p increases manifoldly to attain a value of 2% of the total shift. The techniques for calculating QED corrections for ep and μp are identical, since both the electron and the muon are leptons. Consequently, the measurement of the Lamb shift in muonic hydrogen makes it possible to determine with high accuracy the corrections related to the finite size of the nucleus even if experimental accuracy is moderate.

Experiments in which the 2S–2P transition in muonic hydrogen was searched for were conducted with the πE5 beam of the proton accelerator at PSI. Beginning in 2000, several experimental attempts were made which succeeded in 2010. A special line was created for the experiment to produce slow (∼ 5 keV) muons, which ensures a higher efficiency of muon capture in gaseous hydrogen (pressure 1 mbar) than that for conventional muon beams [40]. Muon capture results in the production of muon-hydrogen atoms in a highly excited state ($n \approx 14$). Most of the atoms rapidly decay into the ground 1S state [41], while about 1% populate the metastable 2S state. After a 0.9-μs-long delay, during which all cascade decays from upper levels are completed, the atoms are irradiated with a short laser pulse at wavelength $\lambda \approx 6$ μm. This results in the excitation of the atoms and their transition from the 2S state to the 2P state, which immediately decays into the ground 1S state (lifetime of the 2P state $\tau = 8.5$ ps) with the emission of an X-ray photon at a wavelength of 0.65 nm. The experiments searched for the resonance that corresponds to the 2S–2P transition by retuning the laser radiation wavelength and measuring the detection rate of the photons with a wavelength of 0.65 nm emitted synchronously with the laser pulse (Fig. 5).

The lifetime of the 2S state in muonic hydrogen in the absence of collisions is 2.2 μs, but under the conditions of the experiment it is reduced to 1 μs due to collisional quenching by gaseous H_2. Consequently, a dedicated pulse laser system is required, which is described in detail in [39]. A continuous tunable titanium-sapphire oscillator pumped by double-frequency radiation of a disc Yb:YAG laser [42, 43] was used. The radiation was converted in a three-cascade Stokes converter based on a vibrational transition in a high-pressure H_2 cell. Laser radiation frequencies were gauged using spectra of water absorption in the wavelength range $\lambda \approx 6$ μm.

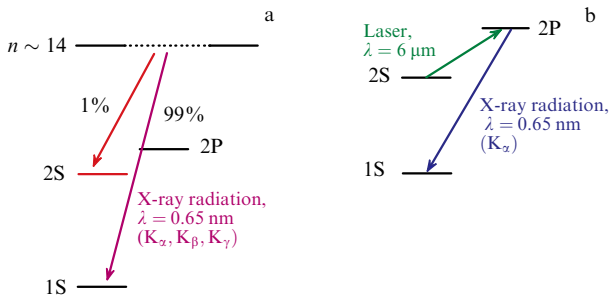

Figure 5. (Color online.) Diagrams of levels and concept of an experiment on muonic hydrogen. (a) After the muon is captured in highly excited states ($n \sim 14$), 99% of population rapidly move in a cascade process to the ground 1S state emitting K-series X-ray radiation (violet arrow). 1% of atoms remain in the metastable 2S state (red arrow). (b) μp atoms in the metastable 2S state are irradiated with a laser pulse (green arrow) at wavelength $\lambda = 6.01$ μm after 0.9 ms, and K_α photons emitted in the decay of the 2P level are detected.

Several experiments carried out in 2003 through 2009, in which the 2S–2P transitions were searched for in the setup described above, failed. In the opinion of the authors, the main reason for the absence of signals was insufficient statistics; significant effort was made to improve the laser system (power enhanced, 'light trap' for radiation with $\lambda = 6$ μm improved) and the detection system. It was only in 2010 that Pohl's team succeeded in detecting a reliable signal and measuring the difference between the energies of the $2S_{1/2}^{F=1}$ and $2P_{3/2}^{F=2}$ states [39]. It was a surprise for the authors that the position of the resonance significantly differed (by several of its spectral widths) from the expected value calculated using the QED technique and the r_p value taken from the tables published at that time by CODATA [44].

Figure 6 shows the 2S–2P resonance in muonic hydrogen. Data were approximated by the Lorenz function taking into consideration the background. The obtained frequency of the transition for the hyperfine centroid was 49881.88(70) GHz and the resonance frequency was 18.0(2.2) GHz. The error in determining both of these quantities corresponds to a statistical error of 1σ. The systematic error of the measurements, equal to 300 MHz, as reported by the authors, is primarily related to gauging of the excitation laser wavelength using water absorption lines in the 5.49–6.01-μm range (one of the lines is also displayed in Fig. 6). The position of these lines is known with an absolute accuracy of 1 MHz [45].

The proton charge radius was determined using the total difference of energies LS_{2S}^{μ} between the $2S_{1/2}^{F=1}$ and $2P_{3/2}^{F=2}$ states in muonic hydrogen, which can be found using the formula

$$LS_{2S}^{\mu} = 50.7725(12)\,\text{THz} - 1.2637 r_p^2\ \text{THz} + 0.0839 r_p^3\ \text{THz}\,, \tag{20}$$

where r_p is measured in femtometers. Consequently, a new value of the proton charge radius was calculated: $r_p = 0.84184(36)(56)$ fm. The first error corresponds to the experimental error, while the second is due to the error of the first term in Eqn (20).

The obtained value of r_p proved to be 10 times more accurate than the CODATA-2006 value, but significantly smaller (by five combined standard deviations) (see Fig. 6). The first assumption, namely an error in QED calculations for muonic hydrogen, was almost immediately rejected, since the 'missing' correction corresponds to 0.31 meV or 64σ in the

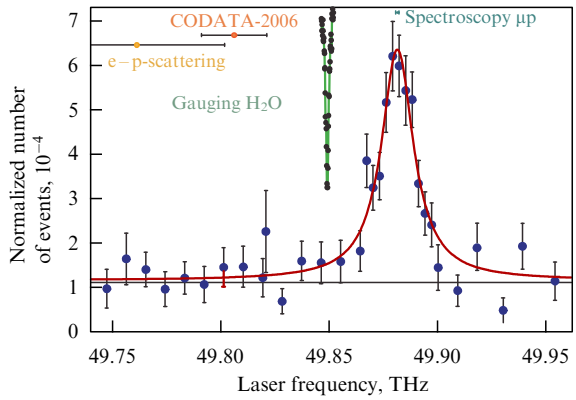

Figure 6. (Color online.) 2S–2P resonance in muonic hydrogen. Blue dots show the number of detected events with a 0.9-ms delay normalized to the total number of events. Red curve represents approximation using the Lorenz function taking into consideration a flat background. Displayed is the expected position of the resonance calculated using the r_p value recommended by CODATA-2006 (red color) and the value that follows from experiments on electron-proton scattering [23, 46] (orange color). One of the gauging spectra on water is also shown (black dots, green curve). (Plot taken from Ref. [39].)

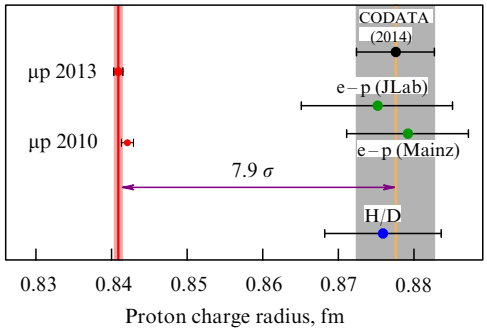

Figure 7. Proton charge radius determined from various experiments. Result obtained by averaging data of the spectroscopy of hydrogen and deuterium (H/D) [80] agrees with data from experiments on elastic electron-proton scattering carried out at Mainz [21] and JLab [22]. The value recommended by CODATA [80] is primarily based on H/D and Mainz group's data. Proton radius obtained using data on muonic hydrogen spectroscopy differs from value recommended by CODATA by 7.9σ.

units of the theoretical error in Eqn (20). The checks that were rapidly made showed that all calculations involve well-known QED corrections and were made properly.

The unexpected result obtained by Pohl's team outlined the problem, which was later named the 'proton radius puzzle' and has been actively discussed for the last decade. Many explanations, including fantastic ones, have been suggested. Some of them are presented in Section 5.

5. Proton charge radius puzzle

The r_p value recommended by the CODATA group has been obtained as a result of analysis of all available experimental data and determination (using QED calculations [31]) of the average r_p and R_∞ values with corresponding errors. Once every four years, the CODATA group revises the recommended values of all fundamental constants based on new experimental data and refined calculations. The averaging method is fully justified provided data do not disagree with each other within the corresponding errors and are described by Gaussian statistics. However, such an approach failed in the case of results for r_p from experiments with muonic hydrogen due to too large a disagreement. CODATA made a decision not to include new results in the analysis until the situation is refined. The experiment with muonic hydrogen was repeated in 2013 with a smaller error, but the disagreement persisted (Fig. 7).

Despite a profound understanding of the processes that occur in measurements of the Lamb shift in μp, attempts were made first to resolve the puzzle invoking effects not taken into account in experiments. For example, study [47] explored the idea that molecular $p\mu e^-$ ions are formed in the process of muon capture. Indeed, the additional electron located at distance a_0 from the μp atom in the 2S state creates an electric field sufficient to shift the observed μp(2S – 2P) line by the required 0.3 meV. It was shown later in [48, 49] that there are no long-lived $p\mu e^-$ systems. Thus, this hypothesis proved to be unlikely.

Possible errors in theoretical calculations were also explored. For example, attempts were made to explain the paradox by a difference in the proton structure in muonic and normal hydrogen. It was hypothesized that the puzzle can be resolved by an anomalously large value of the third-order Zemach correction [50]. This conjecture was later rejected, and it was shown that the third-order Zemach correction — even taking into consideration the refined parametrization of proton form factors — is limited by a value that only exceeds the one obtained for the proton dipole form factor by a factor of two [51]. For the puzzle to be solved, this difference should be larger than 15-fold.

Other hypotheses, such as a large contribution of proton polarizability in the two-photon exchange with large photon momenta [52–54], were also rejected, since they were confirmed neither by experiment nor by theory [55, 56].

It is of interest to mention a thought experiment in which it is assumed that the proton contains in its interior electron-positron pairs and photons [57]. Electroweak interaction between quarks in the proton is 'switched off', as a result of which the particle becomes electrically neutral but similar in its mass and nuclear properties to the normal proton described by the nonperturbed quantum chromodynamic (QCD) wave function. The electroweak interaction between quarks is then 'switched on' again, as a result of which virtual photons and electron-positron pairs modify the wave function of the proton, which now contains additional photons and electron-positron pairs.

Such a change in the shape of the wave function can be significantly larger than that due to electroweak interaction. This was related to the nonlinear nature of QCD and could not be explained in the QED formalism alone. It is very difficult, if at all possible, to estimate in quantitative terms the density of electron-positron pairs inside the proton; however, their presence is not precluded by any known experiments. Moreover, the presence of photons in the proton is confirmed by experiments on deep inelastic Compton scattering. If electron-positron pairs do exist in the proton, the interaction between the proton and the lepton is driven not only by photon exchange but also by annihilation processes. The effective Hamiltonian results in the emergence of nonvanishing interaction between the bound electron and a sea positron, the lightest of leptons, when their total spin is equal to one. This effect should vanish in muonic hydrogen, since the dominant contribution to sea leptons is provided by

the lightest electron-positron pairs and the corresponding annihilation channel is unavailable.

The most intriguing hypotheses are arguably those related to the failure of the Standard Model, which are based on the fact that the measured anomalous magnetic moment of the muon $(g-2)_\mu$ also disagrees with the Standard Model predictions [58, 59]. Recent experiments at the Fermi National Accelerator Laboratory (Fermilab), in which $(g-2)_\mu$ was obtained, confirmed the results of an experiment carried out at the Brookhaven National Laboratory and increased the disagreement with the theoretical prediction to $4.2\,\sigma$ [60, 61]. It should be noted, however, that, unlike the disagreement in the proton charge radius, which is of the order of 10^{-3}, the relative disagreement in $g-2$ is only 10^{-6}. In spite of this, it was asserted that the proton radius puzzle may be a serious obstacle to a reliable prediction of $(g-2)_\mu$ in the Standard Model [62].

Other explanations beyond the Standard Model have been suggested as well. For example, the difference between the electron and muonic hydrogen was explained in [63, 64] by the contribution to the binding energy of an effective Yukawa-type gravitational potential. Study [65] explored a $(4+n)$-dimensional theory with a modified gravitation which, in the authors' opinion, resolve the puzzle by means of an additional gravitational interaction between the proton and the muon.

As was stressed above, extraction of information on the charge radius of the proton from experimental data on scattering is the most complex technique, the result of which depends on the model employed in the analysis of data. Although in most cases Rosenbluth's approximation function yields a 'large' proton charge radius [21–23, 25, 66–68], the analysis based on dispersion relations provided for a long time a 'small' value that corresponds to the result for muonic hydrogen [26, 69–71]. The calculation made in [72] using the effective field theory (EFT) also yielded a small proton radius. The disagreement between the results for muonic and electronic hydrogen encouraged the emergence of studies of various details of fitting functions and approximation techniques [14, 25, 73], some of which yielded a small radius, even if Rosenbluth's fitting function was used [76]. It became apparent that the proton charge radius puzzle cannot be solved without additional experimental data.

6. Muonic deuterium

One option to verify the validity of the measurements in muonic systems is to determine the Lamb shift in muonic deuterium. Indeed, both hydrogen and deuterium are well-studied systems, owing to which the characteristics of the proton and deuterium can be compared. For example, high-precision measurements of the isotopic shift of the 1S–2S transition between H and D, which were made as part of a close scientific collaboration between Lebedev Physical Institute of the Russian Academy of Sciences (FIAN) and the Max Planck Institute for Quantum Optics (MPQ) [77], enabled determining the difference between the charge radii of deuteron and the proton [78]:

$$r_{\rm d}^2 - r_{\rm p}^2 = 3.82007\ {\rm fm}^2\,. \tag{21}$$

The CREMA collaboration (Charge Radius Experiment with Muonic Atoms) planned to conduct a similar comparison in muonic systems by measuring the Lamb shift in muonic deuterium. Although the experiments with muonic hydrogen and muonic deuterium were conducted at the same period of time (2009–2010), interpretation of the results obtained for the muonic deuterium required more than five years. The stumbling point was the deuteron polarizability calculated by K Pachucki [75]. Frequencies for three resonances in μd were reported in 2016 [74]: $2{\rm S}_{1/2}^{F=3/2} \to 2{\rm P}_{3/2}^{F=5/2}$, $2{\rm S}_{1/2}^{F=1/2} \to 2{\rm P}_{3/2}^{F=3/2}$, and $2{\rm S}_{1/2}^{F=1/2} \to 2{\rm P}_{3/2}^{F=1/2}$. A combination of these frequencies and the theoretical values of the fine splitting of the 2P level and the hyperfine splitting of the $2{\rm P}_{3/2}$ level were used to determine the Lamb shift and the hyperfine splitting of the 2S level in the muonic deuterium:

$$L_{2{\rm S}}^{\rm d,\,exp} = 49.05583(75)_{\rm stat}(29)_{\rm syst}\ {\rm THz}\,, \tag{22}$$

$$E_{\rm HFS}^{\rm d,\,exp} = 1.5172(17)_{\rm stat}(5)_{\rm syst}\ {\rm THz}\,, \tag{23}$$

and $E_{\rm HFS}^{\rm exp}$ agrees well with the theoretical prediction for $E_{\rm HFS}^{\rm theo} = 1.5183(12)$ THz [79].

The Lamb shift in μd is very sensitive to the deuteron charge radius, whose contribution is 14%. The obtained value of the deuteron charge radius [74],

$$r_{\rm d}(\mu{\rm d}) = 2.12562(13)_{\rm exp}(77)_{\rm theo}\ {\rm fm}\,, \tag{24}$$

again significantly differs (by 7.5σ) from the value adopted by the CODATA group, $r_{\rm d}({\rm CODATA}) = 2.1424(21)$ fm [80]. An additional comparison of the spectroscopic data on deuterium and muonic deuterium [81] also indicates a significant difference between deuteron radii.

It turns out that the comparison between the H–D and μp – μd systems yields consistent results within each isotopic pair; however, there is no consistency between the electronic and muonic systems. Thus, the unresolved proton radius puzzle has been extended to the deuteron.

7. New measurements of proton radius based on the spectroscopy of normal hydrogen

7.1 Spectroscopy of the single-photon 2S–4P transition using a cryogenic beam

As part of long-term scientific cooperation between FIAN and Hänsch's laboratory at MPQ (Garching, Germany), high-precision spectroscopy experiments began in 2011 to measure single-photon transitions from the metastable 2S state to the $4{\rm P}_{1/2}$ and $4{\rm P}_{3/2}$ states in the hydrogen atom as an attempt to find a solution to the proton radius puzzle. The high-precision measurement of the frequency of the 1S–2S transition carried out by the same joint team [87] was used as an 'anchor value' in using Eqn (15), which requires that no fewer than two transitions be measured.

A spectroscopic method was proposed that essentially differs from the earlier experimental techniques described in Section 3. In contrast to the excitation to the metastable 2S state performed by the electron impact in other experiments on the spectroscopy of the $2{\rm S}-n{\rm S}$, $n{\rm P}$, and $n{\rm D}$ state, the MPQ experiment used for this excitation the optical method of two-photon absorption. This technique makes it possible to employ a cryogenic beam of metastable hydrogen in a particular hyperfine state (in this case, $F=0$). The method requires a system of two-photon 1S–2S excitation (243 nm) featuring an extremely stable frequency, which only became possible after 2010 owing to progress in methods of stabilization of laser sources [83–85]. The system provided a facility to

detect various velocity groups up to 70 m s^{-1}, which enabled a thorough analysis of the systematic effect in conducting 2S–4P spectroscopy, namely, the Doppler effect [86]. Direct measurement of the optical frequency of transitions using a femtosecond optical comb [87] was also used.

The experimental setup was as follows: a beam of atomic hydrogen from a cryogenic nozzle maintained at a temperature of 5.8 K was directed into the area where the 1S–2S transition was excited within an optical cavity, which generated a standing wave (243 nm). The atoms in the 2S state entered the area where the 2S–4P transition was excited. To minimize the Doppler effect, this transition was also excited in a standing light wave (486 nm) with the wave vector orthogonal to the direction in which the atomic beam propagated. In the process of the decay of the 4P level, excited atoms emitted Ly$-\gamma$-photons at a wavelength of 97 nm, which knocked out secondary electrons from the detector walls. The electrons were collected and detected using a secondary electron multiplier.

The contribution from quantum interference of spontaneously emitted photons proved in this experiment to be unexpectedly strong. Despite a large difference between the energies of fine $4P_{1/2}$ and $4P_{3/2}$ sublevels (more than 100 intrinsic widths), the adjacent sublevel makes a significant contribution to the decay amplitude and results in the extension of the resonance under observation to 50 kHz with the statistic error in the determination of the line center of about 2 kHz. Prior to this experiment, this effect had actually not been taken into account in the spectroscopy of atomic transitions [89]. A 'blind' data analysis was used that allows the results not be disclosed until final verification of all systematic effects. Thus, a psychological effect that could affect the final value despite the intentions of the researchers was ruled out.

The methods described above made it possible to reduce the error in the determination of the absolute frequency of the 2S–4P transition centroid to 2 kHz [88], a value that corresponds to the errors of all averaged global data obtained earlier. Consequently, the proton radius calculated based on the frequencies of the 1S–2S and 2S–4P transitions was

$$r_{\mathrm{p}} = 0.8335(95)\ \mathrm{fm}\,, \tag{25}$$

in good agreement with the muonic hydrogen radius but 3.3σ smaller than the value derived from the entire set of global hydrogen data obtained earlier.

It should be noted that each value obtained from measurements in hydrogen conducted in previous years agrees fairly well with the result for muonic hydrogen, and significant disagreement only emerges after averaging. It can be hypothesized that earlier data proved to be correlated due to an unaccounted systematic effect or for psychological reasons in processing data. A candidate for the unaccounted systematic effect may be, for example, the quantum interference phenomenon mentioned earlier or the effect of electric fields in the impact excitation of the hydrogen. The consistency of the obtained result with those for muonic hydrogen, although a surprise, was the first significant step towards solving the proton puzzle.

7.2 Measurement of the Lamb shift in hydrogen

Hessel's team at York University (Canada) carried out in 2014–2019 a new measurement of the Lamb shift L_{2S} in normal hydrogen to obtain a new value of r_{p}. Their approach was based on the conventional technique of radio frequency spectroscopy on a hydrogen beam with a number of modifications.

The measurements used a fast (1% of the speed of light) beam of hydrogen atoms created when protons passed through a molecular hydrogen target. About 4% of the atoms were in the metastable $2S_{1/2}$ state with equal populations of hyperfine sublevels $F = 0$ and $F = 1$. Residual protons were filtered out when the beam passed between 70-cm-long deflecting plates. To separate atoms in the $F = 0$ state, two radio frequency cavities were used which converted atoms from the $2S_{1/2}(F = 1)$ state to the $2P_{1/2}$ state, which rapidly decayed into the ground 1S state.

To measure the frequency of the transition $2S_{1/2}(F{=}0) \to 2P_{1/2}(F{=}1)$, the method of spectroscopy in spaced fields with frequency variation, an analog of the Ramsey method, was used [90]. The residual population of the $2S_{1/2}(F = 0)$ after filtering of the states was determined by applying a constant electric field that mixes the $2S_{1/2}$ and $2P_{1/2}$ levels. The atoms relax into the ground state, emitting Ly$-\alpha$-photons with a wavelength of 121.6 nm, which photo ionize acetone molecules in the detector [91]. An interesting feature of the experiment is that the radio frequency unit could rotate as a whole around the vertical axis. This feature made it possible to change the sequence of the electromagnetic field and to reliably control in this way systematic effects.

The proton charge radius obtained in this experiment was

$$r_{\mathrm{p}} = 0.833(10)\ \mathrm{fm}\,. \tag{26}$$

This result agrees well with both the results for muonic hydrogen and the new result for the spectroscopy of the 2S–4P transition.

8. Two-photon 1S–3S spectroscopy

Biraben's team at the Laboratoire Kastler Brossel (Paris) published in 2018 results of the next measurement of the frequency of the two-photon 1S–3S transition in which the accuracy of the proton charge radius was improved [92]. It should be noted that most of the data that were taken into account by the CODATA group for the optical spectroscopy of highly excited states of the hydrogen atom until 2010 were also obtained by Biraben's team.

The main techniques used in this study were essentially the same as in the earlier experiments of the group. The 1S–3S transition was excited by a continuously operated laser at a wavelength of 205 nm, after which a fluorescence signal from the decay of hydrogen atoms from the 3S state to the 2P state was detected. Experiments were carried out using a thermal beam of atomic hydrogen excited to the 2S state by electronic impact. It should be stressed that the use of a continuously operating laser at this wavelength results in significant engineering problems related to fast degradation of nonlinear converters and optical devices. The authors of [92] reported a significant decrease in error (in comparison to that in their earlier results) in the determination of the absolute frequency of the transition, to 2.7 kHz. The published value of the proton radius $r_{\mathrm{p}} = 0.877(13)$ fm corresponded to that recommended by CODATA, which added ambiguity to the proton puzzle.

Finally, Hänsch's group at MPQ conducted in 2020 another experiment on high-precision spectroscopy of the 1S–3S transition in the hydrogen atom [93]. The concept of the experiment was qualitatively different from that of the

French team. It was based on direct spectroscopy of two-photon transitions using the frequency comb proposed by Baklanov and Chebotaev [94]. The comb is a set of equidistant, mutually coherent optical frequencies with a fixed space between them, $\omega_k = k\omega_r + \omega_0$ (k is an integer), which is generated by a laser with mode synchronization. The pulse repetition frequency ω_r and the offset frequency $\omega_0 < \omega_r$ can be accurately measured. The two-photon 1S–3S transition is excited when two comb pulses moving in opposite directions are superimposed; the energies of the photons from different modes add in such a way that their total energy corresponds to the transition energy $\hbar\omega_{1S\text{–}3S}$. If the condition $2\omega_k = \omega_{1S\text{–}3S}$ holds for one of the modes, the condition of the two-photon resonance is automatically fulfilled for all other pairs of the modes: $\omega_{1S\text{–}3S} = \omega_{k-m} + \omega_{k+m}$, and the excitation occurs in a coherent way.

The primary advantage of this method over continuous excitation is that the pulsed radiation can be efficiently converted into the ultraviolet range. In this case, similar to the continuous radiation regime, the entire radiation power is involved in excitation of the transition. The list of disadvantages includes the residual Doppler effect due to the broad spectrum of the comb, the chirp effect, and the small excitation volume that is controlled by the pulse duration and the constriction radius.

The authors of [93] used the frequency of the transition $1S(F = 1) \to 3S(F = 1)$ taking into consideration hyperfine splitting to obtain the frequency of the centroid of the 1S–3S transition with an accuracy which is 3.6 times better that that in the French group's experiment. The proton radius calculated using the frequency of the 1S–2S and 1S–3S transitions was

$$r_p = 0.8482(38)\,\text{fm}\,, \tag{27}$$

which proved to be 2.9σ smaller than the value derived from the set of global hydrogen data obtained before 2014, including the most recent measurement of the frequency of the 1S–3S transition [92]. The difference from the value that follows from muonic hydrogen is 1.9σ.

A conclusion can be drawn that the most recent experiments listed in this section confirm the results obtained in studying muonic systems and actually solve the charge radius puzzle indicating the problems in hydrogen experiments of earlier generations.

9. Conclusions

Although the hydrogen atom is well studied and the simplest atomic system, it still involves a number of unresolved problems that can perplex researchers. Two allegedly absolutely independent methods — elastic scattering of electrons on protons and the spectroscopy of hydrogen — provided reliable coincidence of the results, which could not raise doubts among scientists. It was only a significant increase in experimental accuracy due to the use of muonic systems that resulted in rethinking all earlier results that had been collected for more than 50 years.

Figure 8 shows the values of the proton charge radius obtained in different years. One can see in the figure that before 1980 the only source of information about the proton radius was experiments on elastic scattering of electrons on protons. The declared accuracy was at that early time not high, and the results were not in disagreement with those for

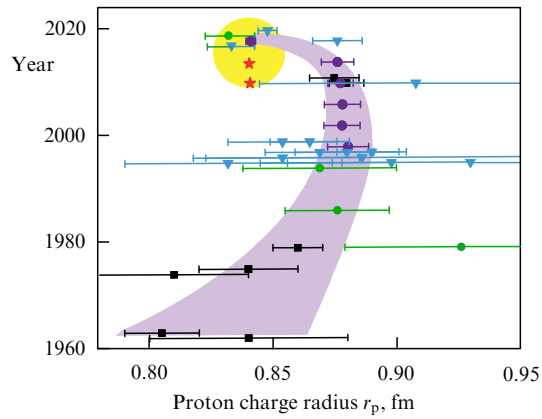

Figure 8. (Color online.) Retrospective representation of proton charge radius using various measuring techniques. Black squares show results of experiments on elastic e–p-scattering; green dots, RF measurements of the Lamb shift in hydrogen; red stars, results of muonic hydrogen spectroscopy; and violet dots, value of the proton radius recommended by CODATA. Values are taken from review [96]. Violet band shows how the generally accepted value of the proton radius changed and the error in determining its value decreased. Yellow dot highlights the group of experiments whose results led to a shift of the recommended proton charge radius to smaller values.

muonic hydrogen. The situation changed later when high-precision methods of hydrogen atom spectroscopy emerged and, before 2014, the r_p value recommended by CODATA was closer to 0.88 fm.

On the other hand, in the Standard Model, the electron in no way differs from the muon except in mass, and the same QED formalism can be applied to both particles. Consequently, the value $r_p \approx 0.84$ fm obtained in 2010 in experiments with muonic hydrogen was kind of a shock in atomic physics. More than a decade was needed to clarify the issue, and it can be asserted today that the Standard Model passed the test. Figure 8 shows that, beginning in 2010, data are separated into two groups that disagree with each other. CODATA had to make a difficult decision in favor of one of the groups in 2018 [95]. Taking into account the independent character and variety of methods, CODATA gave preference to muonic experiments and recommended the following values:

$$r_p = 0.8414(19)\,\text{fm}\,, \tag{28}$$

$$R_\infty c = 3.2898419602508(64) \times 10^{15}\,\text{Hz}\,. \tag{29}$$

The relative error in determining the proton charge radius significantly reduced, to 2.2×10^{-3}. An important consequence was also a significant, almost threefold, decrease in the relative error (in comparison to that in 2010) in the Rydberg constant, to 1.9×10^{-12}.

It appears that the proton charge radius puzzle has not only scientific but also psychological origins related to processing data and selecting the methods that provide 'synchronization' with the allegedly generally accepted value and concurrently with the desire to show the best result. This may include the underestimation of errors, exclusion of allegedly 'poor quality' experimental points, incomplete or insufficiently unbiased analysis of systematic effects, and the selection of an appropriate model for processing data. Moreover, the data obtained by one group of researchers or

at one experimental facility using similar methods should be critically reviewed from the perspective of possible correlations, including those that are related to unidentified systematic errors. Straightforward averaging methods may prove to be inapplicable. The proton charge radius puzzle was a good lesson and at the same time a perfect driver for progress in experimental and theoretical studies of simple atomic systems.

Acknowledgments
This study was supported by the Russian Foundation for Basic Research (grant no. 20-12-50101).

References

1. Karshenboim S G *Phys. Usp.* **56** 883 (2013); *Usp. Fiz. Nauk* **183** 935 (2013)
2. Biraben F *Eur. Phys. J. Spec. Top.* **172** 109 (2009)
3. Antognini A et al. *Science* **339** 417 (2013)
4. Hofstadter R, Bumiller F, Yearian M R *Rev. Mod. Phys.* **30** 482 (1958)
5. Hofstadter R *Annu. Rev. Nucl. Sci.* **7** 231 (1957)
6. Hofstadter R, McAllister R W *Phys. Rev.* **98** 217 (1955)
7. McAllister R W, Hofstadter R *Phys. Rev.* **102** 851 (1956)
8. Yennie D R, Lévy M M, Ravenhall D G *Rev. Mod. Phys.* **29** 144 (1957)
9. Rosenbluth M N *Phys. Rev.* **79** 615 (1950)
10. Walecka J D *Nuovo Cimento* **11** 821 (1959)
11. Ernst F J, Sachs R G, Wali K C *Phys. Rev.* **119** 1105 (1960)
12. Bernauer J C et al. (A1 Collab.) *Phys. Rev. C* **90** 015206 (2014)
13. Barcus S K, Higinbotham D W, McClellan R E *Phys. Rev. C* **102** 015205 (2020)
14. Punjabi V et al. *Eur. Phys. J. A* **51** 79 (2015)
15. Higinbotham D W et al. *Phys. Rev. C* **93** 055207 (2016)
16. Lehmann P, Taylor R, Wilson R *Phys. Rev.* **126** 1183 (1962)
17. Hand L N, Miller D G, Wilson R *Rev. Mod. Phys.* **35** 335 (1963)
18. Murphy J J (II), Shin Y M, Skopik D M *Phys. Rev. C* **9** 2125 (1974)
19. Borkowski F et al. *Nucl. Phys. B* **93** 461 (1975)
20. Simon G G et al. *Nucl. Phys. A* **333** 381 (1980)
21. Bernauer J et al. (A1 Collab.) *Phys. Rev. Lett.* **105** 242001 (2010)
22. Zhan X et al. *Phys. Lett. B* **705** 59 (2011)
23. Sick I *Phys. Lett. B* **576** 62 (2003)
24. Sick I, Trautmann D *Phys. Rev. C* **89** 012201 (2014)
25. Hill R J, Paz G *Phys. Rev. D* **82** 113005 (2010)
26. Lorenz I T, Hammer H-W, Meißner U-G *Eur. Phys. J. A* **48** 151 (2012)
27. Lorenz I T, Meißner U-G *Phys. Lett. B* **737** 57 (2014)
28. Mohr P J, Newell D B, Taylor B N *Rev. Mod. Phys.* **88** 035009 (2016)
29. Parker R H et al. *Science* **360** 191 (2018)
30. Heiße F et al. *Phys. Rev. Lett.* **119** 033001 (2017)
31. Eides M I, Grotch H, Shelyuto V A *Phys. Rep.* **342** 63 (2001)
32. Pohl R et al. *Hyperfine Interactions* **127** 161 (2000)
33. Meyer V et al. *Phys. Rev. Lett.* **84** 1136 (2000)
34. Horbatsch M, Hessels E A *Phys. Rev. A* **93** 022513 (2016)
35. Lundeen S R, Pipkin F M *Phys. Rev. Lett.* **46** 232 (1981)
36. Hagley E W, Pipkin F M *Phys. Rev. Lett.* **72** 1172 (1994)
37. van Wijngaarden A, Holuj F, Drake G W *Can. J. Phys.* **76** 95 (1998)
38. de Beavoir B et al. *Eur. Phys. J. D* **12** 61 (2000)
39. Pohl R et al. *Nature* **466** 213 (2010)
40. Antognini A et al. *AIP Conf. Proc.* **796** 253 (2005)
41. Pohl R et al. *Hyp. Interact.* **193** 115 (2009)
42. Antognini A et al. *IEEE J. Quantum Electron.* **45** 993 (2009)
43. Giesen A et al. *Appl. Phys. B* **58** 365 (1994)
44. Mohr P J, Taylor B N, Newell D B *Rev. Mod. Phys.* **80** 633 (2008)
45. Toth R A *J. Mol. Spectrosc.* **190** 379 (1998)
46. Blunden P G, Sick I *Phys. Rev. C* **72** 057601 (2005)
47. Jentschura U D *Ann. Physics* **326** 516 (2011)
48. Karr J-P, Hilico L *Phys. Rev. Lett.* **109** 103401 (2012)
49. Umair M, Jonsell S *J. Phys. B* **47** 175003 (2014)
50. De Rújula A *Phys. Lett. B* **693** 555 (2010)
51. Cloët I C, Miller G A *Phys. Rev. C* **83** 012201 (2011)
52. Miller G A et al. *Phys. Rev. A* **84** 020101 (2011)
53. Hill R J, Paz G *Phys. Rev. Lett.* **107** 160402 (2011)
54. Miller G A *Phys. Lett. B* **718** 1078 (2013)
55. Miller G A, Thomas A W, Carroll J D *Phys. Rev. C* **86** 065201 (2012)
56. Birse M C, McGovern J A *Eur. Phys. J. A* **48** 120 (2012)
57. Jentschura U D *Phys. Rev. A* **88** 062514 (2013)
58. Bennet G W et al. (Muon g–2 Collab.) *Phys. Rev. D* **73** 072003 (2006)
59. Hagiwara K et al. *J. Phys. G* **38** 085003 (2011)
60. Abi B et al. (Muon g–2 Collab.) *Phys. Rev. Lett.* **126** 141801 (2021)
61. Aoyama T et al. *Phys. Rep.* **887** 1 (2020)
62. Karshenboim S G, McKeen D, Pospelov M *Phys. Rev. D* **90** 073004 (2014)
63. Onofrio R *Mod. Phys. Lett. A* **28** 1350022 (2013)
64. Onofrio R *Europhys. Lett.* **104** 20002 (2013)
65. Wang L-B, Ni W-T *Mod. Phys. Lett. A* **28** 1350094 (2013)
66. Sick I *Few-Body Syst.* **50** 903 (2014)
67. Ron G et al. (The Jefferson Lab Hall A Collab.) *Phys. Rev. C* **84** 055204 (2011)
68. Lee G, Arrington J R, Hill R J *Phys. Rev. D* **92** 013013 (2015)
69. Belushkin M A, Hammer H-W, Meißner U-G *Phys. Rev. C* **75** 035202 (2007)
70. Adamuscin C, Dubnicka S, Dubnickova A Z *Prog. Part. Nucl. Phys.* **67** 479 (2012)
71. Lorenz I T et al. *Phys. Rev. D* **91** 014023 (2015)
72. Bauer T, Bernauer J C, Scherer S *Phys. Rev. C* **86** 065206 (2012)
73. Kraus E et al. *Phys. Rev. C* **90** 045206 (2014)
74. Pohl R et al. *Science* **353** 669 (2016)
75. Pachucki K *Phys. Rev. Lett.* **106** 193007 (2011)
76. Griffioen K, Carlson C, Maddox S *Phys. Rev. C* **93** 065207 (2016)
77. Parthey C G et al. *Phys. Rev. Lett.* **104** 233001 (2010)
78. Jentschura U D et al. *Phys. Rev. A* **83** 042505 (2011)
79. Krauth J J et al. *Ann. Physics* **366** 168 (2016)
80. Mohr P J, Taylor B N, Newell D B *Rev. Mod. Phys.* **84** 1527 (2012)
81. Pohl R et al. *Metrologia* **54** (2) L1 (2017)
82. Parthey C G et al. *Phys. Rev. Lett.* **107** 203001 (2011)
83. Alnis J et al. *Phys. Rev. A* **77** 053809 (2008)
84. Kolachevsky N N, Khabarova K Yu *Phys. Usp.* **57** 1230 (2014); *Usp. Fiz. Nauk* **184** 1354 (2014)
85. Kolachevsky N N *Phys. Usp.* **47** 1101 (2004); *Usp. Fiz. Nauk* **174** 1171 (2004)
86. Beyer A et al. *Ann. Physik* **525** 671 (2013)
87. Udem Th, Holzwarth R, Hänsch T W *Nature* **416** 233 (2002)
88. Beyer A et al. *Science* **358** 79 (2017)
89. Udem Th et al. *Ann. Physik* **531** 1900044 (2019)
90. Vutha A C, Hessels E A *Phys. Rev. A* **92** 052504 (2015)
91. Bezginov N et al. *Science* **365** 1007 (2019)
92. Fleurbaey H et al. *Phys. Rev. Lett.* **120** 183001 (2018)
93. Grinin A et al. *Science* **370** 1061 (2020)
94. Baklanov E V, Chebotaev V P *Sov. J. Quantum Electron.* **7** 1252 (1977); *Kvantovaya Elektron.* **4** 2189 (1977)
95. National Institute of Standards and Technology U.S. Department Commerce. The Physical Measurement Laboratory (PML), https://physics.nist.gov/
96. Karr J-P, Marchand D, Voutier E *Nat. Rev. Phys.* **2** 601 (2020)